Electrochemical CO_2 Reduction to Alcohols Using Flexible and Rigid MOF Electrocatalysts

Rodrigo Andrés Espinosa-Flores[a], Martin Daniel Trejo-Valdez[a,*], María Elena Manríquez-Ramírez[a,**], Francisco Javier Tzompantzi-Morales[b], Hugo Martínez-Gutiérrez[c], Milla-Vikberg[d], Tanja Kallio[d] and Arturo Susarrey-Arce[e]

[a.]Instituto Politécnico Nacional, ESIQIE, Laboratorio de investigación en nanomateriales y energías limpias, Edificio Z-5, P.B., Zacatenco, Gustavo A. Madero, Ciudad de México, 07738, México. e-mail: mtrejov@ipn.mx; mmanriquez@ipn.mx

[b.]Departamento de Química, Área de Catálisis, Universidad Autónoma Metropolitana – Iztapalapa, Av. San Rafael Atlixco No. 189, 09340 Ciudad de México, México.

[c.]Centro de Nanociencias y Micro y Nanotecnologías-Instituto Politécnico Nacional, Unidad Profesional Adolfo López Mateos, Av. Luis Enrique Erro s/n, Gustavo a Madero, 07738 Mexico City, Mexico.

[d.]Department of Chemistry and Materials Science, Aalto University School of Chemical Engineering, Kemistintie 1, 02015 Espoo, Finland.

[e.]Department of Chemical Engineering, Mesoscale Chemical Systems, MESA+ Institute, University of Twente, P.O. Box 217, Enschede 7500 AE, The Netherlands

[*]Corresponding author: mtrejov@ipn.mx

[**]Corresponding author: mmanriquez@ipn.mx

1. XPS

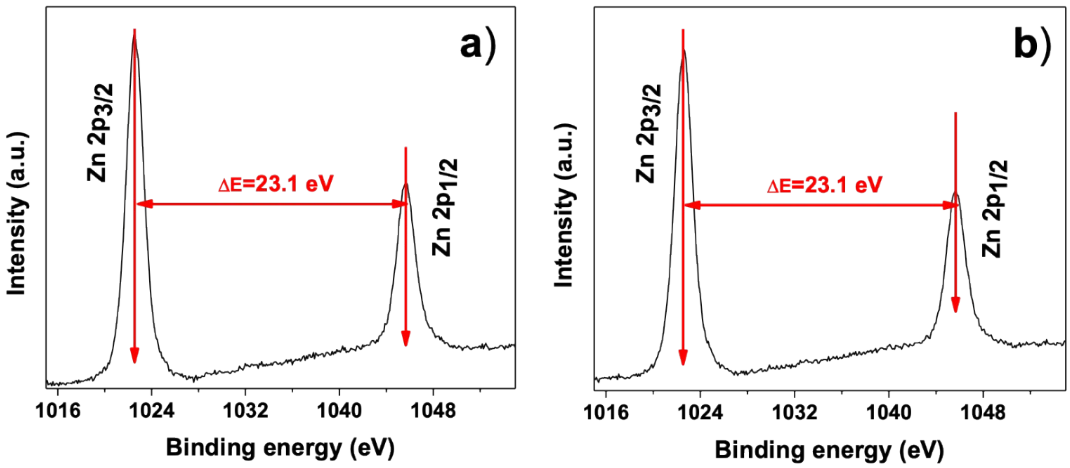

Fig. S1. Core XPS spectra of Zn 2p. (a) H_4DOBDC MOF and b) Oxalic acid MOF.

2. Calculation of specific capacitance and ECSA

For a given capacitor, it is found that the amount of charge Q acquired by each plate is proportional to the magnitude of the potential difference V between them:

$$Q = CV \tag{1-1}$$

The constant of proportionality, C, in the above equation is called the capacitance of the capacitor. The following equation can determine the capacitance of a given capacitor:

$$C = \frac{Q}{V} \tag{1-2}$$

By dividing by the mass of active material in grams, m, we obtain the specific capacitance, C_s, given by,

$$C_s = \frac{Q}{mV} \tag{1-3}$$

The average current, I, is defined as,

$$I = \frac{Q}{t} \tag{1-4}$$

Or,

$$Q = I * t \tag{1-5}$$

Replacing equation (1-5) in equation (1-3) we get,

$$C_s = \frac{I * t}{mV} \tag{1-6}$$

Dividing the numerator and denominator by t,

$$C_s = \frac{I}{m(\frac{V}{t})} \tag{1-7}$$

In equation (1-7), (V/t) represents cyclic voltammetry scan rate, which will be abbreviated as a constant, k.

$$C_s = \frac{I}{mk} \tag{1-8}$$

Or,

$$I = C_s * m * k \tag{1-9}$$

Considering the cyclic voltammetry experiments, the current in the range potential from V_a to V_b. Therefore, equation (1-9) can be written in its integral form as,

$$\int_{V_a}^{V_b} I\,(V)dV = \int_{V_a}^{V_b} (C_s * m * k)dV \qquad (1\text{-}10)$$

Or,

$$Area = \int_{V_a}^{V_b} (C_s * m * k)dV \qquad (1\text{-}11)$$

The values of Cs, m, and k are constant for a specific material. Therefore, the integral of equation (1-11) can be solved as,

$$Area = (V_b - V_a) * C_S * m * k \qquad (1\text{-}12)$$

When the capacitor is charging, then Area=A_1 and equation (1-12) can be written as,

$$A_1 = (V_b - V_a) * C_S * m * k \qquad (1\text{-}13)$$

Similarly, when the capacitor is discharging, then Area=A_2 and equation (1-12) can be written as,

$$A_2 = (V_a - V_b) * C_s * m * k \qquad (1\text{-}14)$$

For the calculation of the Area inside the cyclic voltammetry curve, equation (1-14) must be subtracted from equation (1-13),

$$Area = A_1 - A_2 = \left[(V_b - V_a) * C_S * m * k\right] - \left[(V_a - V_b) * C_s * m * k\right]$$

$$Area = A_1 - A_2 = \left[(V_b - V_a) * C_S * m * k\right] + \left[(V_b - V_a) * C_s * m * k\right]$$

$$Area = A_1 - A_2 = 2\left[(V_b - V_a) * C_S * m * k\right] \qquad (1\text{-}15)$$

Solving the equation (1-15) ultimately involves isolating C_s to determine its equation.

$$C_s = \frac{Area}{2(V_b - V_a) * m * k} \qquad (1\text{-}16)$$

Where C_s is the specific capacitance in F/g, Area has units in A*V, m is the mass of active materials, k is the scan rate in volts per second, and V_b—V_a is the potential window of cyclic voltammetry.

The respective Cs and the corresponding ECSA calculation for H_4DOBDC MOF and oxalic acid MOF are shown below, respectively. Given m=10 mg (0.01 g) and k=10 mV×s^{-1} (0.01 V×s^{-1}),

$$C_s = \frac{1.3295\ A * V}{2 * (0.1973\ V) * 0.01\ g * 0.01\ V \times s^{-1}} = 33{,}700.01\ \frac{A \times s}{V \times g} = 33{,}700.01 \frac{F}{g}$$

$$C_s = \frac{1.5365\ A * V}{2 * (0.1949\ V) * 0.01\ g * 0.01\ V \times s^{-1}} = 39{,}419.03\ \frac{A \times s}{V \times g} = 39{,}419.03 \frac{F}{g}$$

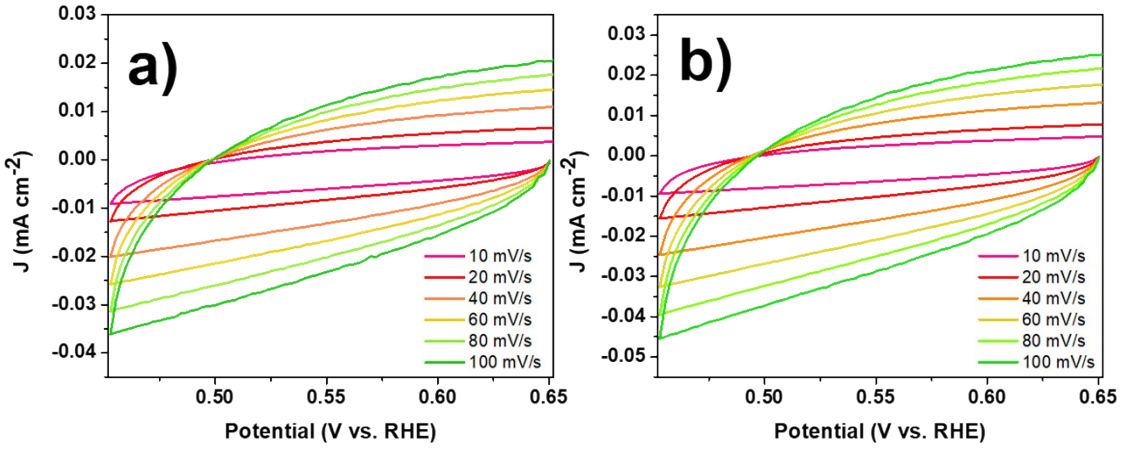

Fig. S2. Cyclic voltammograms (CVs) of a) H_4DOBDC MOF and b) Oxalic acid MOF in CO_2-saturated 0.1 M KOH electrolyte at various scan rates.

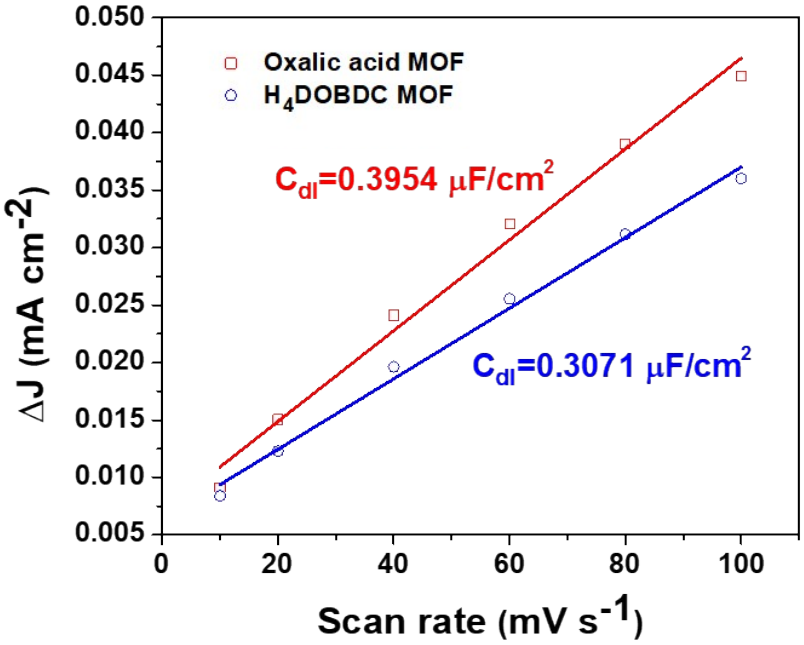

Fig. S3. Average current density against the scan rate showing the double-layer capacitance (C_{dl}) extracted from the corresponding CVs presented in **Fig. S3**.

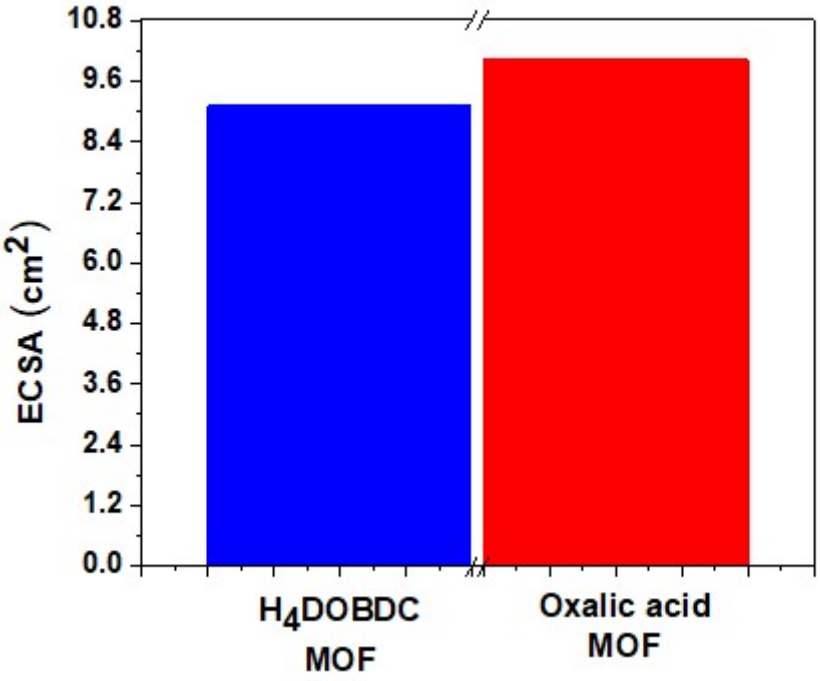

Fig. S4. The estimated electrochemical surface area for H_4DOBDC MOF and Oxalic acid MOF.

3. Chronoamperometry

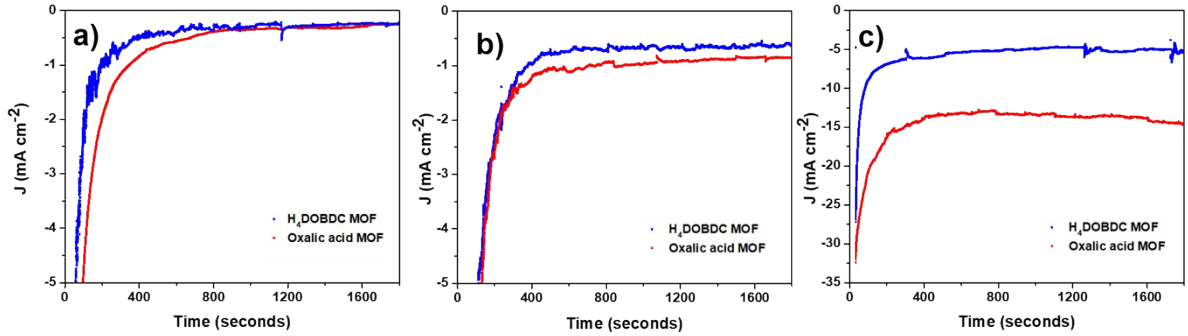

Fig. S5. Chronoamperometry curves recorded in CO_2-saturated 0.1 M KOH electrolyte for the MOFs at: a) -0.19 V vs RHE, b) -0.59 V vs RHE, and c) -1.01 V vs RHE.

Table S1. Comparison of the faradic efficiency (FE) of the present work, oxalic acid MOF, and other materials in the literature.

Electrocatalysts Metals/Metal Oxides	**Reaction product**	**Electrolyte**	**Faradic efficiency**	**Potential (V vs. RHE)**	**Ref.**
Cu_4Zn	EtOH	0.1 M $KHCO_3$	30%	–1.05	[1]
ZnO-CuO	EtOH	0.1 M $KHCO_3$	32%	–1.15	[2]
Cu-ZnO	iPrOH	0.1 M $KHCO_3$	33.65%	–0.99	[3]
CuAg alloy	iPrOH	CO_2-saturated $CsHCO_3$	39.6%	–0.73	[4]
MOFs	**Reaction product**	**Electrolyte**	**Faradic efficiency**	**Potential (V vs. RHE)**	**Ref.**
Carbonized HKUST-1 (OD Cu/C-1000)	EtOH	0.1 M $KHCO_3$	34.8%	–0.5	[5]
Cu-based MOF	EtOH	0.5 M $KHCO_3$	82.5%	–1.0	[6]
CuSn-based MOF (CuSn-HAB)	EtOH	1 M KOH	56%	–0.57	[7]
Oxalic acid MOF	EtOH	0.1 M KOH	15.02%	–0.19	This work
Oxalic acid MOF	iPrOH	0.1 M KOH	29.09%	–0.19	This work

4. Product distribution from an H-cell

For the analysis of gaseous products, an H-cell with two compartments (cathode, anode) and a water jacket for temperature control was used. A Pt mesh cylinder served as a counter electrode in the anode compartment, while an XR300 Ag/AgCl reference electrode (Radiometer Analytical) and a CT carbon cloth with MPL (W1S1011) gas diffusion electrode with the painted catalyst acted as the reference and working electrodes, respectively, in the cathode compartment. The gas diffusion electrode was prepared by spray painting a catalyst ink containing ca. 12 mg of MOF catalyst and 220 µL of 5 wt.% Nafion ionomer (1:1 MOF catalyst-to-ionomer ratio by weight) in 400 µL of isopropanol plus 100 µL of MQ-H_2O. The ink was prepared by 15 minutes of ultrasonication in an ultrasound bath and overnight stirring. The ink was sprayed on a 4 cm diameter area using a PTFE template using a Badger model 100G airbrush. The painted electrode was left to dry overnight in a desiccator. The loading of MOF catalyst was consistently 0.7±0.01 mg cm^{-2}, determined by weighing the electrode before and after painting. The active area of the working electrode was 12.56 cm^2.

For each cell compartment, 80 mL of 0.1 M $KHCO_3$ aqueous solution served as both anolyte and catholyte. The temperature was maintained at 25 °C with water circulation in the water jacket whilst the electrolyte was stirred in the cathode compartment at 350 rpm with a magnetic stirrer. A Nafion 115 membrane separated the two liquid compartments. CO_2 was bubbled into the cathode compartment at 10-13 mL min^{-1} and directed to analysis in micro gas chromatography (Agilen 990) through the catholyte compartment and a rotameter. Before CO_2 reduction, the system was stabilized for 30 minutes under CO_2 flow before running 1 baseline GC chromatogram to ensure removal of residual H_2, O_2, and N_2 and to ensure the system was not leaking. CO_2 reduction was performed by chronoamperometry (CA) at desired applied potential (–0.72 V, –0.99 V, and –1.40 V vs. RHE) for 4 h, and gas chromatograms were recorded every 30 minutes. Electrochemical impedance spectroscopy (EIS) was recorded between 20 kHz and 1 Hz at 10 mV amplitude before and after bulk CO_2 reduction to determine solution resistance for iR correction. The potentials reported for gaseous products analysis were corrected by the iR drop, and the potentials were reported versus RHE according to the following formula: $E_{RHE} = (E_{Ag/AgCl} — iR) + 0.2 + 0.059*pH$;

Where $E_{Ag/AgCl}$ is the applied potential (V), i is the current (A), and R is the solution resistance determined by EIS (Ω). The gaseous products were monitored online with an Agilent 990-micro GC. The Faradaic efficiency of gaseous products was determined using the following formula: $FE_{Gas}=(z*F*\varphi_{Gas}*\upsilon_m/i_{tot})*100\%$, where z is the number of electrons transferred to produce a particular gaseous product (for H_2 = 2e⁻, and CO = 2e⁻), F is Faraday's constant (96485.3 C mol^{-1}), φ_{Gas} is the volume of the gas product determined by GC, υ_m is the molar

flow rate of CO_2 gas determined with the rotameter (mol s^{-1}). The liquid products ($HCOO^-$) were quantified with HPLC using the following formula: $FE_{Liquid}=(z*F*c_{Liquid}*V/i_{tot}*t)*100\%$.

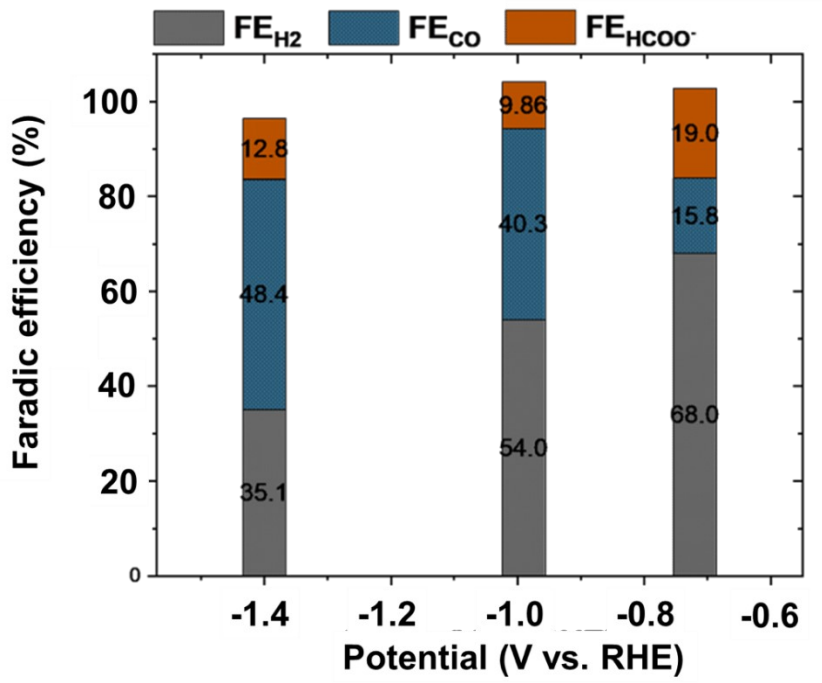

Fig. S6. Faradic efficiency (%) in CO_2-saturated 0.1 M $KHCO_3$ using the H-cell with H_4DOBDC MOF at -0.72 V vs RHE, -0.99 V vs RHE, and -1.40 V vs RHE.

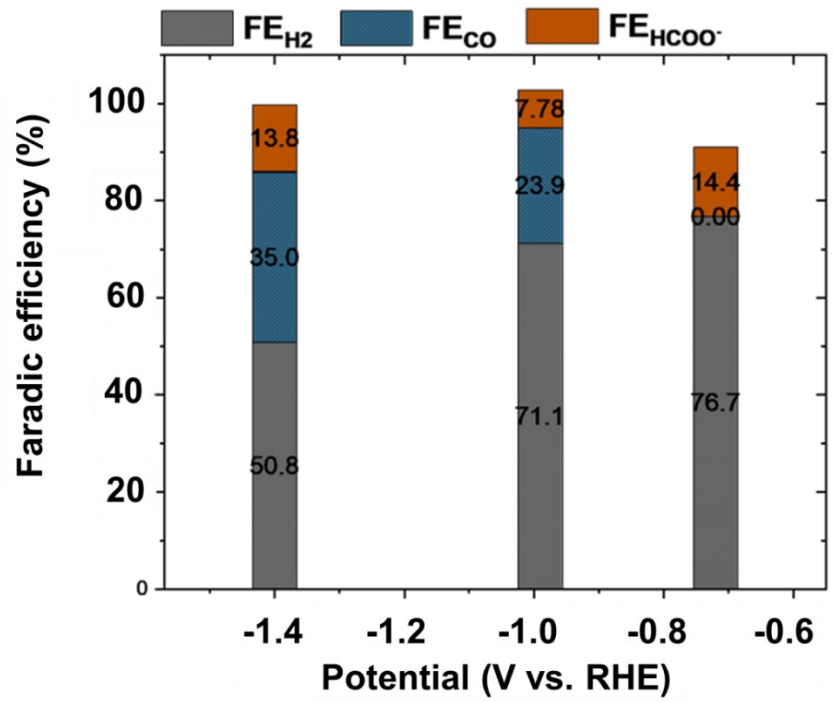

Fig. S7. Faradic efficiency (%) in CO_2-saturated 0.1 M $KHCO_3$ using the H-cell with oxalic acid MOF at -0.72 V vs RHE, -0.99 V vs RHE, and -1.40 V vs RHE.

4. Electrocatalyst Stability

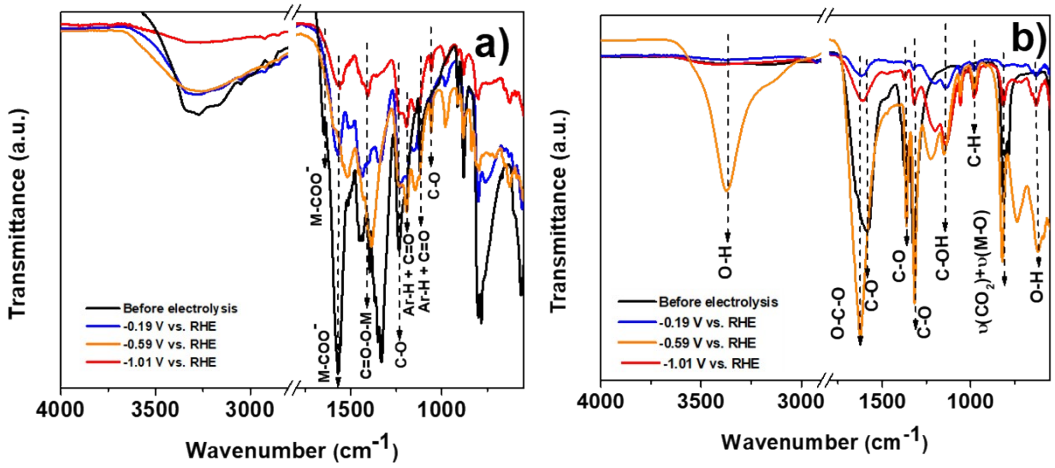

Fig. S8. FTIR spectra comparison for the MOFs before and after the chronoamperometric tests (at -0.19 V, -0.59 V, and -1.01 V vs. RHE). a) H_4DOBDC MOF and b) Oxalic acid MOF.

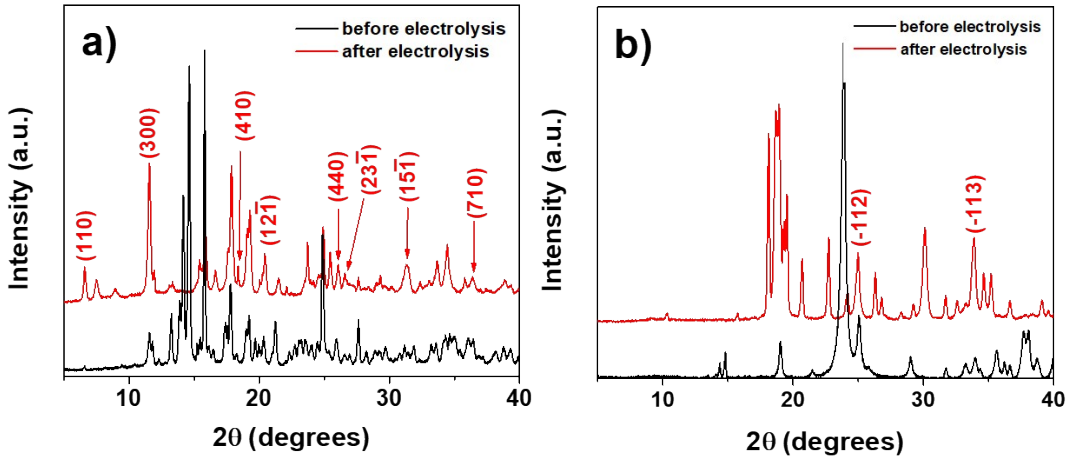

Fig. S9. MOF XRD patterns before and after electrolysis at -0.19 V vs. RHE. a) H_4DOBDC MOF and b) Oxalic acid MOF.

5. TGA

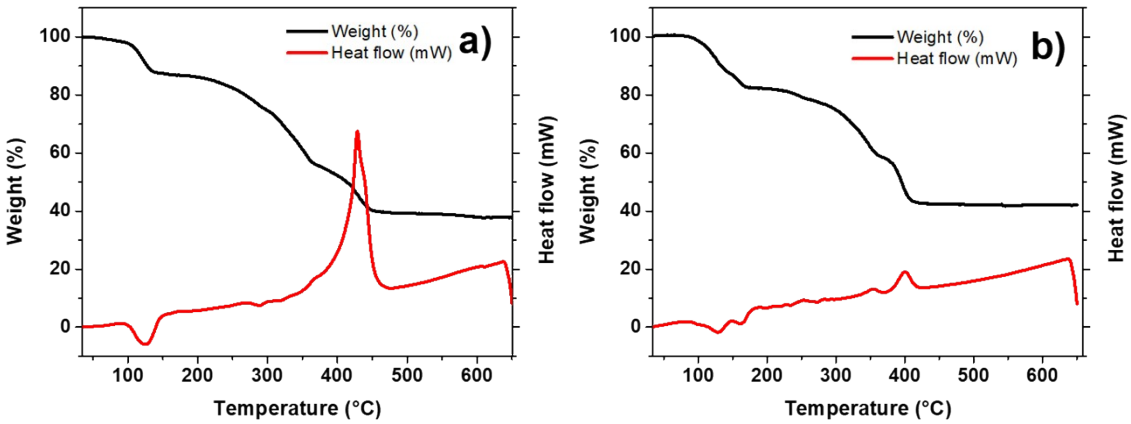

Fig. S10. TGA curves of: a) H_4DOBDC MOF and b) Oxalic acid MOF.

6. Electrocatalyst Stability: Chronoamperometry

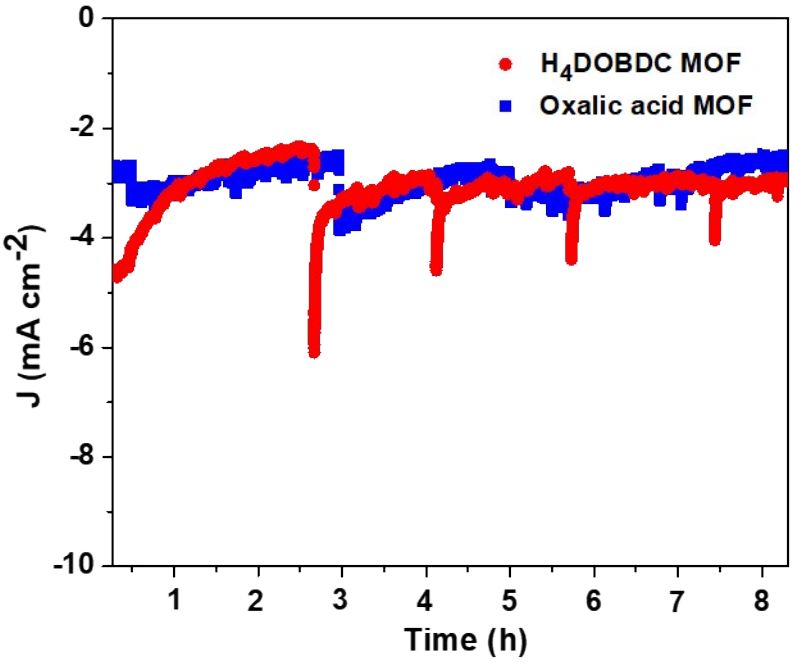

Fig. S11. Chronoamperometry stability tests in CO_2-saturated 0.1 M KOH electrolyte for 8h at –1.01 V vs. RHE. a) H_4DOBDC MOF and b) Oxalic acid MOF.

References

(1) Ren, D.; Su-Hui Ang, B.; Siang Yeo, B. Tuning the Selectivity of Carbon Dioxide Electroreduction toward Ethanol on Oxide-Derived Cu_xZn Catalysts. ACS Catal. 2016, 6, 12, 8239-8247.

(2) Ren, J. Gao, L. Pan, Z. Wang, J. Luo, S. M. Zakeeruddin, A. Hagfeldt, M. Gratzel. Atomic Layer Deposition of ZnO on CuO Enables Selective and Efficient Electroreduction of Carbon Dioxide to Liquid Fuels. Angew. Chem. Int. Ed. 2019, 58, 15036–15040.

(3) Munir, S.; Amir, R. V.; Sarp, K. (2018). Electrocatalytic reduction of CO_2 to produce higher alcohols. Sustainable Energy & Fuels, 2, 2532-2541.

(4) K. Qi, Y. Zhang, N. Onofrio, E. Petit, X. Cui, J. Ma, J. Fan, H. Wu, W. Wang, J. Li, J. Liu, Y. Zhang, Y. Wang, G. Jia, J. Wu, L. Lajaunie, C. Salameh, D. Voiry, Unlocking direct CO_2 electrolysis to C_3 products via electrolyte supersaturation. Nat. Catal. 2023, 6, 319–331.

(5) Zhao, K.; Liu, Y.; Quan, X.; Chen, S.; Yu, H. CO_2 electroreduction at low overpotential on oxide-derived Cu/carbons fabricated from metal organic framework. Acs. Appl. Mater. Interfaces, 2017, 9, 5302–5311

(6) Shao, B.; Du, H.; Rui-Kang, H.; Xing-Lu, H.; Yan, L.; Yi-Lei, X.; Lin-bin, J.; Min, D.; Shixiong, L.; Zhong, Z.; Jin, H. Metal–Organic Framework Supported Low-Nuclearity Cluster Catalysts for Highly Selective Carbon Dioxide Electroreduction to Ethanol. Angewandte Chemie, 2024, 63, 45, e202409270.

(7) Zhen-Hua, Z.; Jia-Run, H.; Pei-Qin, L.; Xiao-Ming, C. Highly Efficient Electroreduction of CO_2 to Ethanol via Asymmetric C–C Coupling by a Metal–Organic Framework with Heterodimetal Dual Sites. J. Am. Chem. Soc., 2023, 145, 49, 26783-26790.